Journal of Molecular Spectroscopy 259 (2010) 70–79

Contents lists available at ScienceDirect

Journal of Molecular Spectroscopy

journal homepage: www.elsevier.com/locate/jms

# Equilibrium structure in the presence of internal rotation: A case study of *cis*-methyl formate

J. Demaison [a,*], L. Margulès [b], I. Kleiner [c], A.G. Császár [d]

[a] Laboratoire de Chimie quantique et Photophysique, CP160/09, Université Libre de Bruxelles (U.L.B.), Ave. F.D. Roosevelt, 50, B-1050 Brussels, Belgium
[b] Laboratoire de Physique des Lasers, Atomes et Molécules, UMR CNRS 8523, Université de Lille I, 59655 Villeneuve d'Ascq Cedex, France
[c] Laboratoire Interuniversitaire des Systèmes Atmosphériques (LISA), CNRS UMR 7583 et Universités Paris 7 et Paris 12, 61 av. du Général de Gaulle, 94010 Créteil, Cédex, France
[d] Laboratory of Molecular Spectroscopy, Institute of Chemistry, Eötvös University, H-1518 Budapest 112, P.O. Box 32, Hungary

ARTICLE INFO

*Article history:*
Received 24 September 2009
In revised form 2 November 2009
Available online 18 November 2009

*Keywords:*
*Ab initio*
Equilibrium structure
Semi-experimental
Internal rotation
Methyl formate

ABSTRACT

The Born–Oppenheimer (BO) equilibrium molecular structure ($r_e^{BO}$) of *cis*-methyl formate has been determined at the CCSD(T) level of electronic structure theory using Gaussian basis sets of at least quadruple-ζ quality and a core correlation correction. The quadratic, cubic and semi-diagonal quartic force field in normal coordinates has also been computed at the MP2 level employing a basis set of triple-ζ quality. A semi-experimental equilibrium structure ($r_e^{SE}$) has been derived from experimental ground-state rotational constants and the lowest-order rovibrational interaction parameters calculated from the *ab initio* cubic force field. To determine $r_e^{SE}$ structures, it is important to start from accurate ground-state rotational constants. Different spectroscopic methods, applicable in the presence of internal rotation and used in the literature to obtain "unperturbed" rotational constants from the analysis and fitting of the spectrum, are reviewed and compared. They are shown to be compatible though their precision may be different. The $r_e^{BO}$ and $r_e^{SE}$ structures are in good agreement showing that, in the particular case of *cis*-methyl formate, the methyl torsion can still be treated as a small-amplitude vibration. The best equilibrium structure obtained for *cis*-methyl formate is: $r(C_m–O) = 1.434$ Å, $r(O–C_c) = 1.335$ Å, $r(C_m–H_s) = 1.083$ Å, $r(C_m–H_a) = 1.087$ Å, $r(C_c–H) = 1.093$ Å, $r(C{=}O) = 1.201$ Å, $\angle(COC) = 114.4°$, $\angle(CCH_s) = 105.6°$, $\angle(CCH_a) = 110.2°$, $\angle(OCH) = 109.6°$, $\angle(OCO) = 125.5°$, and $\tau(H_aCOC) = 60.3°$. The accuracy is believed to be about 0.001 Å for the bond lengths and 0.1° for the angles.



## 1. Introduction

Methyl formate, $HCOOCH_3$, exists in two different conformers, a so-called *cis* and a so-called *trans* forms. The energy difference between them is large, $\Delta H = 4.75(19)$ kcal mol$^{-1}$ as obtained by infrared spectroscopy in an Ar matrix [1]. Until very recently only the *cis* conformer (the methyl group *cis* to the C=O bond, see Fig. 1) has been observed in the gas phase. The laboratory spectrum and an interstellar detections of the *trans* methyl formate conformer were in fact reported this year [2].

*Cis*-methyl formate (CMF) may be considered as a prototypical molecule for studying the internal rotation of the methyl group. The potential hindering the internal rotation is not high, $V_3 = 372.672(4)$ cm$^{-1}$ [3]; thus, it produces large splittings of the rotational transitions, even in the ground torsional state. Other advantages of CMF are that its *A* rotational constant is rather small [3] and that two components of the electric dipole moment are significantly different from zero, $\mu_a = 1.63$ D and $\mu_b = 0.68$ D [4]. The latter fact permits the measurement of many transitions, including high-*J* transitions ($J \leqslant 80$). On the other hand, the density of the spectrum is increased by the existence of several low-lying vibrations (torsion around 130 cm$^{-1}$, COC bend at 318 cm$^{-1}$, and an out-of-plane bend at 332 cm$^{-1}$) [5] and its assignment is thus not straightforward. Furthermore, it is difficult to obtain a good fit of all transitions because some splittings are very large and the molecule is non-rigid. The most recent fit [3] included 10533 transitions and required 67 parameters. The first study of the microwave spectrum is due to Curl [4] and a short review of the microwave history of CMF is given in Ref. [3].

CMF is also an important interstellar molecule. It was first detected towards SgrB2 in 1975 [6], it was then found ubiquitous and it is known as an interstellar "weed" due to its dense radioastronomical spectrum [7,8]. This prompted new spectroscopic studies of CMF, see again Ref. [3] for a review. The analysis of the first excited torsional state led to the assignment of several new lines towards Orion KL [9]. More recently, the measurements of the spectra of the $H^{13}COOCH_3$, $HCOO^{13}CH_3$ [10], and $DCOOCH_3$ [11] isotopologues permitted the identification of these species in Orion.

* Corresponding author. Fax: +33 3 20 33 70 20.
*E-mail address:* jean.demaison@univ-lillel.fr (J. Demaison).

0022-2852/$ - see front matter © 2009 Elsevier Inc. All rights reserved.
doi:10.1016/j.jms.2009.11.007

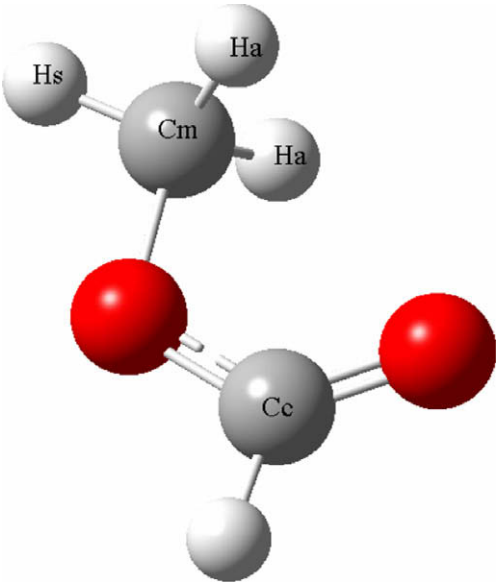


**Fig. 1.** *cis*-Methyl formate.

As the rotational spectra of many isotopologues of CMF have been recently analyzed in great detail furnishing very accurate rotational constants, it seemed worth investigating whether an accurate equilibrium structure can be determined for CMF. The experimental gas-phase structure of CMF was first determined by Curl [4] using the rotational constants of eight isotopologues. Assuming that the methyl group is symmetrical with its axis through the carbon, he was able to obtain a substitution ($r_s$) structure. More recently, another experimental structure was determined by gas electron diffraction furnishing $r_a$ parameters with an assumed accuracy of 0.002–0.003 Å for the distances between heavy atoms and 0.5° for the bond angles [12]. Several *ab initio* equilibrium structures have been determined but the most accurate one [13] seems to have been determined at the second-order Møller–Plesset perturbation theory level (MP2) [14] with a basis set of quadruple zeta quality.

This paper is organized as follows. Section 2 describes the *ab initio* calculation of the Born–Oppenheimer equilibrium structure of CMF. In Section 3, its *ab initio* anharmonic force field is discussed and some parameters calculated from this force field are compared to the corresponding experimental values. Section 4 focuses on the experimental determination of reliable ground-state rotational constants. Depending on the method chosen, the internal rotation analysis leads to the determination of different sets of rotational constants which are apparently incompatible. This has produced some confusion and a clarification is obviously needed. In this paper, we focus on the methods and codes previously used in the literature for analyzing and fitting the microwave and millimeterwave spectra of CMF. The usefulness of the pseudo-inertial defect is also discussed. Section 5 is devoted to the semi-experimental equilibrium structure. Finally, Section 6, the experimental internal rotation parameters are compared to the values calculated from the equilibrium structure.

## 2. *Ab initio* structure

As part of this study the molecular geometry of CMF has been optimized at the coupled cluster (CC) level of electronic structure theory including single and double excitations [15] augmented by a perturbational estimate of the effects of connected triple excitations [CCSD(T)] [16] in conjunction with the correlation-consistent polarized valence *n*-tuple-zeta basis sets, cc-pV*n*Z (abbreviated hereafter as V*n*Z), with $n \in \{D(2), T(3), Q(4), 5\}$ [17]. It is well established that the CCSD(T) technique usually provides reliable equilibrium structures [18] though exceptions exist [19]. As it is not obvious that the CCSD(T) structural parameters are converged at the VQZ level, we also used a mixed basis set composed of VQZ on H and V5Z on the other atoms. This basis set, denoted V(5,Q)Z, leads to little loss in accuracy and reduces the computation time. To further reduce computational cost, the V(5,Q)Z basis was employed only with MP2 [14]. The frozen-core approximation (hereafter denoted as fc), i.e., keeping the 1s orbitals of C and O doubly occupied during correlated-level calculations, was used in most calculations. To estimate the inner-shell correlation effects, the weighted correlation-consistent polarized core-valence *n*-tuple zeta (wCV*n*Z) [20,21] basis sets were also employed at the MP2 level. For first-row atoms this correction is substantial [22] but it is sufficient to use the MP2 method to estimate its magnitude [23]. The CCSD(T) calculations were performed with the MOLPRO program package [24], while the MP2 calculations utilized the Gaussian03 (g03) program [25].

At the MP2 level, enlargement of the basis set from VTZ to VQZ shows that convergence is almost achieved for the CH bond lengths and the CCH bond angles, but there are non-negligible changes for the CO bond lengths, the $C_{[carbonyl]}$–O bond being shortened by as much as 0.0034 Å, see Table 1. Upon going from VQZ to V(5,Q)Z, still at the MP2 level, the $C_{[carbonyl]}$–O bond length decreases very slightly by 0.0006 Å and the $C_{[methyl]}$–O bond length by 0.0003 Å indicating that convergence is almost achieved. As O is electronegative, diffuse functions play a significant role when the basis set is small but it is well established that their effect rapidly decreases with the size of the basis set and should be, thus, negligible at the V5Z level [26]. To check this point, we have calculated the structure at the MP2 level using the aug-cc-pVQZ (abbreviated as AVQZ) basis set [27]. Going from VQZ to AVQZ, the effects are small, the largest ones being an increase of the $C_{[methyl]}$–O bond length by 0.0017 Å and of the C=O bond length by 0.0012 Å. Correlating all electrons at the MP2/wCVQZ level leads to the expected shortening of the bonds: 0.0015 Å for CH, 0.0030 Å for C–O, and 0.0022 Å for C=O. The best *ab initio* $r_e^{BO}$ structure is obtained by adding this core correlation correction to the CCSD(T)/VQZ structure and by taking into account the effects caused by the basis set enlargement (MP2/cc-pVQZ → MP2/cc-pV(5,Q)Z), except for the CH bond lengths. This structure is given at the right of Table 1 (estimate I). As the effect of the diffuse functions was neglected, the CO bond lengths might be slightly too small. Alternatively, taking into account also the effect of diffuse functions at the quadruple zeta level leads to estimate II. In this case, the CO bond lengths are probably slightly too large.

## 3. *Ab initio* anharmonic force field

The *ab initio* anharmonic force field [28] of CMF was calculated in normal coordinates at the MP2 level of theory using the g03 program [25]. It is widely accepted that, in most cases, the CCSD(T) force field only provides a negligible improvement over the MP2 force field when determining semi-experimental equilibrium structures [29]. The VTZ basis set was used in the frozen-core approximation and also with all electrons correlated. The optimized molecular geometry was calculated first. Then, the associated harmonic force field was evaluated analytically in Cartesian coordinates at the optimized geometry in order to avoid the non-zero force dilemma [30]. The cubic ($\phi_{ijk}$) and semi-diagonal quartic ($\phi_{ijkk}$) normal coordinate force constants were determined with the use of a finite difference procedure involving displacements [31] along reduced normal coordinates and the calculation of analytic second derivatives at these displaced geometries. Evaluation of the anharmonic spectroscopic constants was based on second-order rovibrational perturbation theory [32].

**Table 1**
*Ab initio* Born–Oppenheimer estimates of the equilibrium structure of *cis*-methyl formate (bond lengths in Å, angles in degrees).

| Method | MP2 | | | | | | | CCSD(T) | $r_e^{BO}$ | |
|---|---|---|---|---|---|---|---|---|---|---|
| Basis set [a] | VTZ | VTZ(ae) | VQZ | V(Q,5)Z | AVQZ | wCVQZ | wCVQZ(ae) | VQZ | I[b] | II[c] |
| $r(C_m–O)$ | 1.4362 | 1.4313 | 1.4343 | 1.4346 | 1.4360 | 1.43402 | 1.43095 | 1.4366 | 1.4338 | 1.4355 |
| $r(O–C_c)$ | 1.3400 | 1.3355 | 1.3366 | 1.3360 | 1.3370 | 1.3363 | 1.3336 | 1.3375 | 1.3343 | 1.3347 |
| $r(C_m–H_s)$ | 1.0829 | 1.0797 | 1.0818 | 1.082 | 1.0821 | 1.0817 | 1.0801 | 1.0850 | 1.0834 | 1.0837 |
| $r(C_m–H_a)$ | 1.0863 | 1.083 | 1.0852 | 1.0855 | 1.0856 | 1.0851 | 1.0836 | 1.0883 | 1.0868 | 1.0872 |
| $r(C_c–H)$ | 1.0931 | 1.0883 | 1.0923 | 1.0928 | 1.0926 | 1.0923 | 1.0909 | 1.0945 | 1.0931 | 1.0934 |
| $r$(C=O) | 1.2056 | 1.2026 | 1.20355 | 1.20357 | 1.2047 | 1.2032 | 1.2100 | 1.2019 | 1.1997 | 1.2008 |
| ∠(COC) | 113.785 | 113.888 | 114.038 | 114.119 | 114.088 | 114.043 | 114.125 | 114.197 | 114.360 | 114.411 |
| $\angle(CCH_s)$ | 105.574 | 105.676 | 105.537 | 105.498 | 105.481 | 105.545 | 105.619 | 105.593 | 105.628 | 105.572 |
| $\angle(CCH_a)$ | 110.365 | 110.400 | 110.259 | 110.202 | 110.167 | 110.259 | 110.290 | 110.244 | 110.217 | 110.125 |
| ∠(OCH) | 109.092 | 109.191 | 109.261 | 109.334 | 109.345 | 109.273 | 109.324 | 109.444 | 109.569 | 109.653 |
| ∠(OCO) | 125.708 | 125.689 | 125.597 | 125.555 | 125.539 | 125.594 | 125.578 | 125.583 | 125.525 | 125.467 |
| $\tau(H_aCOC)$ | −60.307 | −60.297 | −60.295 | −60.285 | −60.284 | −60.290 | −60.278 | −60.281 | −60.259 | −60.248 |

[a] Frozen core approximation unless otherwise stated, ae = all electrons correlated. m stands for methyl, c for carbonyl, s for symmetric (in-plane) and a for asymmetric (out-of-plane), see Fig. 1.
[b] Estimate I: CCSD(T)/VQZ + MP2[V(Q,5)Z − VQZ + wCVQZ(ae) − wCVQZ].
[c] Estimate II: estimate I + MP2/AVQZ − MP2/VQZ.

The experimental torsional ground-state ($v_\tau = 0$) and the computed equilibrium quartic centrifugal distortion constants are compared in Table 2. Generally, this permits a check of the quality of the harmonic part of the force field. There is no significant difference between the different *ab initio* calculations and the agreement is best with the most recent experimental determination of the torsional ground-state $v_\tau = 0$ constants [33]. The centrifugal distortion constants were also determined in Ref. [3] but the method used in that work involved the diagonalization of matrices involving several torsional $v_\tau$ states. Furthermore, they are not derived in the Principal Axis System (PAS). Therefore, the values of the centrifugal distortion constants derived in Ref. [3] cannot be directly compared to the computed constants. It is worth noting the large variation of the $\delta_K$ constant between the different experimental studies but it is known that it is difficult to get accurate values for this constant.

The harmonic vibrational frequencies, $\omega_i$, and the vibrational band centers, $v_i$, for $HCOOCH_3$ are given in Table 3. The agreement between the calculated and the experimental vibrational frequencies $v_i$ is good, the median of the absolute deviations is only 9.6 $cm^{-1}$ (1%) at the MP2/VTZ(fc) level. This is comparable to or even slightly better than the results found for many molecules of this size. At the MP2/VTZ(ae) level, the median of absolute deviations is 20.0 $cm^{-1}$. As usual, the largest deviations are for the CH bond stretches. What is truly interesting is that the deviations are more systematic and that the agreement is much better for the methyl torsional vibration at the MP2/VTZ(ae) level than at the MP2/VTZ(fc) level. The harmonic part of the force field has also been calculated at the MP2/AVTZ level of theory. This does not significantly improve the agreement.

The lowest-order experimental vibration–rotation interaction constants ($\alpha_\tau$) have been determined as

$$\alpha_\tau^A = A(v_\tau = 0) - A(v_\tau = 1) \quad \text{(and identical formula for } \alpha_\tau^B \text{ and } \alpha_\tau^C) \tag{1}$$

for the torsional mode of $HCOOCH_3$ and $H^{13}COOCH_3$ [33]. They are compared with their *ab initio* counterparts in Table 4. This comparison is particularly interesting because, in this molecule, the torsion may be considered as a well isolated mode which is not perturbed by anharmonic resonances, at least for the ground and first torsional states, isolated from the other small-amplitude vibrations, $v_{12}$ (COC bend) located at 318 $cm^{-1}$ and $v_{17}$ (out-of-plane bend) at 332 $cm^{-1}$. On the other hand, torsion is a large-amplitude motion and we would expect that this severely affects the accuracy of the calculated anharmonic force field. At first glance, the agreement is comparable or better than that found for other molecules without large-amplitude motion. Thus, it may be concluded that, in the particular case of CMF, the torsion behaves as a small-amplitude vibration, at least for the ground and first torsional mode $v_\tau = 0$ and 1, which are located very much below the top of the torsional barrier. The question of the accuracy of the experimental $\alpha_\tau$ constants is still pending because even though the $v_\tau = 0$ and 1 torsional states fit to experimental accuracy [3], it is not the case for $v_\tau = 2$ state. The fit of the second excited torsional state will require most likely the inclusion of perturbations with the two low-frequency modes $v_{12}$ and $v_{17}$, which, according to Ref. [3], lie very close to the third excited torsional level and which could therefore affect $v_\tau = 2$ through torsional–rotation interactions. This effect has also been seen in Ref. [33], where the values of $A(v_\tau = 2) - A(v_\tau = 1) = -180.88$ MHz and $B(v_\tau = 2) - B(v_\tau = 1) = 42.96$ MHz are quite far away from the values reported in Table 4.

The next step is to combine the theoretical α-constants deduced from the *ab initio* force field with the experimental ground-state rotational constants to yield the semi-experimental equilibrium

**Table 2**
Experimental and *ab initio* quartic centrifugal distortion constants[a] (kHz) for the ground torsional state of $HCOOCH_3$.

| Method | Experimental | | | | | MP2 | | B3LYP |
|---|---|---|---|---|---|---|---|---|
| Ref./basis | [33] | [55] | [56] | [57] | [58] | VTZ(fc) | VTZ(ae) | VTZ |
| $\Delta_J$ | 6.049 | 5.890 | 6.018 | 6.178 | 6.059 | 6.162 | 6.169 | 6.143 |
| $\Delta_{JK}$ | −21.229 | −23.313 | −27.862 | −17.198 | −21.290 | −21.987 | −22.922 | −22.473 |
| $\Delta_K$ | 77.806 | 75.401 | 85.137 | 82.358 | 79.133 | 73.390 | 74.939 | 84.123 |
| $\delta_J$ | 1.886 | 1.857 | 1.869 | 1.950 | 1.871 | 1.932 | 1.935 | 1.895 |
| $\delta_K$ | 3.939 | 2.057 | 9.815 | 7.660 | 3.951 | 4.990 | 5.627 | 2.973 |

[a] The uncertainty is not given because it is much smaller than the difference between the different values.

**Table 3**
Harmonic frequencies $\omega_i$ and vibrational band centers $\nu_i$ ($cm^{-1}$) for $HCOOCH_3$.

| Mode | Description | Exp.[a] | MP2/VTZ(fc) | | | MP2/VTZ(ae) | | |
|---|---|---|---|---|---|---|---|---|
| | | $\nu_i$ | $\omega_i$ | $\nu_i$ | $\nu_i^{exp} - \nu_i^{calc}$ | $\omega_i$ | $\nu_i$ | e − c |
| $\nu_1(a')$ | $CH_3$ stretch | 3045 | 3228.6 | 3096.9 | −51.9 | 3231.0 | 3096.2 | −51.2 |
| $\nu_2(a')$ | $CH_3$ stretch | 2969 | 3112.2 | 2967.9 | 1.1 | 3119.4 | 3028.1 | −59.1 |
| $\nu_3(a')$ | CH stretch | 2943 | 3100.9 | 3041.1 | −98.1 | 3127.0 | 2978.3 | −35.3 |
| $\nu_4(a')$ | C=O stretch | 1754 | 1792.1 | 1745.7 | 8.3 | 1803.6 | 1772.4 | −18.4 |
| $\nu_5(a')$ | $CH_3$ def | 1454 | 1520.9 | 1495.9 | −41.9 | 1533.4 | 1492.2 | −38.2 |
| $\nu_6(a')$ | $CH_3$ def | 1445 | 1479.8 | 1455.9 | −10.9 | 1489.2 | 1456.0 | −11.0 |
| $\nu_7(a')$ | CH bend | 1371 | 1408.9 | 1376.7 | −5.7 | 1424.4 | 1390.8 | −19.8 |
| $\nu_8(a')$ | C–O stretch | 1207 | 1251.5 | 1209.7 | −2.7 | 1261.4 | 1223.9 | −16.9 |
| $\nu_9(a')$ | $CH_3$ rock | 1166 | 1198.5 | 1171.6 | −5.6 | 1204.5 | 1176.3 | −10.3 |
| $\nu_{10}(a')$ | O–$CH_3$ stretch | 924 | 964.7 | 945.7 | −21.7 | 972.8 | 946.0 | −22.0 |
| $\nu_{11}(a')$ | OCO def | 767 | 777.1 | 768.9 | −1.9 | 782.9 | 773.3 | −6.3 |
| $\nu_{12}(a')$ | COC def. | 318 | 309.9 | 337.0 | −19.0 | 349.2 | 338.3 | −20.3 |
| $\nu_{13}(a'')$ | $CH_3$ stretch | 3012 | 3193.5 | 3053.9 | −41.9 | 3197.0 | 3061.5 | −49.5 |
| $\nu_{14}(a'')$ | $CH_3$ def. | 1443 | 1508.1 | 1466.3 | −23.3 | 1520.7 | 1478.9 | −35.9 |
| $\nu_{15}(a'')$ | CH3 rock | 1168 | 1192.7 | 1170.8 | −2.8 | 1199.2 | 1174.4 | −6.4 |
| $\nu_{16}(a'')$ | CH bend | 1032 | 1054.2 | 1033.4 | −1.4 | 1070.9 | 1044.9 | −12.9 |
| $\nu_{17}(a'')$ | C–O tors. | 332 | 346.9 | 335.2 | −3.2 | 311.8 | 309.4 | 22.6 |
| $\nu_{18}(a'')$ | $CH_3$ tors. | 130 | 148.7 | 190.2 | −60.2 | 161.9 | 139.5 | −9.5 |
| MAD[b] | | | | | 9.6 | | | 20.0 |

[a] Ref. [5].
[b] Median absolute deviation.

**Table 4**
Experimental and *ab initio* (MP2/VTZ) vibration–rotation interaction constants ($\alpha_\tau$)[a] (MHz) for the torsional vibration in $HCOOCH_3$ and $H^{13}COOCH_3$.

| | | Exp.[b] | fc[c] | ae[d] |
|---|---|---|---|---|
| $HCOOCH_3$ | $\alpha^A$ | −119.22 | −114.30 | −105.72 |
| | $\alpha^B$ | 67.08 | 68.93 | 65.03 |
| | $\alpha^C$ | 26.30 | 27.78 | 26.16 |
| $H^{13}COOCH_3$ | $\alpha^A$ | −118.64 | −114.97 | −105.26 |
| | $\alpha^B$ | 66.33 | 67.98 | 64.34 |
| | $\alpha^C$ | 25.94 | 27.76 | 25.79 |

[a] See Eq. (1).
[b] Ref. [33], the uncertainty is not given because it is much smaller than the difference between the experimental and *ab initio* values.
[c] fc = frozen-core approximation.
[d] ae = all electrons correlated.

rotational constants. However, it is first necessary to check the accuracy of the experimentally deduced ground-state constants. This is done in the next section.

## 4. Internal rotation analysis

The internal rotation of a "symmetric" rotor, like the methyl group, generally produces A–E doublet splittings of the rotational transitions. The model generally used to analyze the internal rotation consists of two rigid groups connected by a bond. One of the groups (the top) is quasi-symmetric, close to $C_{3v}$ symmetry (the top rarely has a $C_{3v}$ local point-group symmetry in an asymmetric top, as shown in Table 5, but this constraint is not really necessary

**Table 5**
Structure of a few methyl groups (distances in Å and angles in deg.).[a]

| | $r(CH_s)$ | $r(CH_a)$ | $\angle(XCH_s)$ | $\angle(XCH_a)$ |
|---|---|---|---|---|
| $(CH_3)_2O$[b] | 1.086 | 1.095 | 107.6 | 111.3 |
| $CH_3NH_2$[b] | 1.093 | 1.087 | 115.0 | 109.1 |
| $CH_3OH$[c] | 1.086 | 1.091 | 106.8 | 112.0 |
| $HCOOCH_3$[d] | 1.083 | 1.087 | 105.6 | 110.2 |

[a] s = in-plane, a = out-of-plane.
[b] Ref. [59].
[c] Ref. [60].
[d] This work, see Table 1.

to derive the Hamiltonian [34]). The rigid frame-rigid top Hamiltonian is [35]

$$\mathbf{H} = F(\mathbf{p}_\alpha - \mathbf{P})^2 + V(\alpha) + \mathbf{H}_R, \quad (2)$$

where $\mathbf{H}_R$ is the rotational Hamiltonian, $\mathbf{p}_\alpha$ is the internal rotation angular momentum conjugate to the torsional angle $\alpha$, and

$$\mathbf{P} = \sum_g \rho_g J_g (g = a,\ b,\ c), \quad (3)$$

where $J_g$ is a component of the rotational angular momentum. The $\boldsymbol{\rho}$ vector and the inverse reduced moment of inertia $F$ are defined using $I_{\alpha'}$ the moment of inertia of the top, and $\lambda_a$, $\lambda_b$, and $\lambda_c$, the direction cosines of the internal rotation axis $i$ of the top in the principal axis system, i.e., $\lambda_g = \cos(\angle(i,g))$. The components of $\boldsymbol{\rho}$ are

$$\rho_g = \frac{\lambda_g I_\alpha}{I_g} \quad (4)$$

where $I_g$ are the moments of inertia of the whole molecule in the principal axis system.

The inverse reduced moment of inertia of the top is

$$F = \frac{\hbar^2}{2rI_\alpha} \quad (5)$$

with

$$r = 1 - \sum_g \lambda_g^2 \frac{I_\alpha}{I_g}. \quad (6)$$

The potential corresponding to the methyl internal rotation has a $2\pi/3$ periodicity [35] and is expressed in the usual Fourier series

$$V(\alpha) = \frac{1}{2}[V_3(1 - \cos\ 3\alpha) + V_6(1 - \cos\ 6\alpha) + \cdots] \quad (7)$$

### 4.1. Principal axis method (PAM)

When the principal inertial axis system (PAS) is used as the coordinate system, the inertial tensor of the whole molecule is diagonal, and thus

$$\mathbf{H}_R = AJ_a^2 + BJ_b^2 + CJ_c^2 + \mathbf{H}_{CD}. \quad (8)$$

In Eq. (8), $A$, $B$, and $C$ are the rotational constants in the PAS and $\mathbf{H}_{CD}$ the usual centrifugal distortion Hamiltonian. To the best of our

knowledge, in the methods and codes using purely the PAM, $-2Fp\mathbf{P}$ is considered as a perturbation[1] which can be handled by successive Van Vleck transformations. Consequently, an effective rotational Hamiltonian is obtained for each vibrational state $v$ and internal rotation substate $\sigma = A, E$ [36,37] as

$$\mathbf{H}^{\mathrm{PAM}}_{v\sigma} = \mathbf{H}_{\mathrm{R}} + F\sum_n W^{(n)}_{v\sigma}\mathbf{P}^n + \frac{1}{2}W^{(\mathrm{d})}_{v\sigma}[[\mathbf{P},\mathbf{H}_{\mathrm{R}}],\mathbf{P}]. \tag{9}$$

The coefficients $W^{(n)}_{v\sigma}$ and $W^{(\mathrm{d})}_{v\sigma}$ result from the Van Vleck perturbational treatment. They were tabulated [38] and can be calculated easily [36,39].

The coefficient $W^{(\mathrm{d})}_{v\sigma}$ is worth a comment because it may affect the structure. In the Van Vleck transformations, the denominators are differences of the type $\Delta E = E_{RT} - E_{R'T'}$ where $R$ represents the rotational quantum numbers and $T$ the torsional ones. It is assumed that the rotational contribution to these differences is negligible compared to the torsional contribution, i.e. $\Delta E \approx E_T - E_{T'}$. The error caused by ignoring the smaller rotational contribution can be corrected by expanding the denominators in a Taylor series and this is called the denominator correction. One interesting property of $W^{(\mathrm{d})}_{v\sigma}$ is that it is almost the same for $\sigma = A$ and $\sigma = E$. Thus, it does not significantly contribute to the splittings but it affects the rotational constants. Usually, this denominator correction is not taken into account in the analysis of the spectra but some authors argued that it is important to consider it during an accurate structure determination [40]. However, we propose that it is better to simply neglect it for reasons shown in Section 4.4.

From a fit of the spectrum, the following parameters are usually derived: $A$, $B$, $C$, $V_3$, $I_\alpha$, and the spherical angles $\theta$ and $\varphi$ (or the direction cosines $\lambda_g$) defining the position of the internal rotation axis $i$. In PAM, the $A$ and $E$ torsional levels can be fit separately and each torsional level $v_\tau$ is also fit separately.

For the $A$-levels, $W^{(2n+1)}_{vA} \equiv 0$ [36], hence there are no odd-order terms in the effective Hamiltonian of Eq. (9), and it is possible to fit the $A$-lines to a standard Watson Hamiltonian. The relation between the fitted rotational constants, $A_{vA}$, $B_{vA}$, and $C_{vA}$ and the "unperturbed" rotational constants, $A$, $B$, and $C$ is (correct to fourth order)

$$A_{vA} = A + F\rho_a^2 W^{(2)}_{vA} + F[3\rho_b^2\rho_c^2 - 2\rho_a^2\rho_b^2 - 2\rho_a^2\rho_c^2]W^{(4)}_{vA} + [\rho_b^2(C-A) + \rho_c^2(B-A)]W^{(\mathrm{d})}_{vA} \tag{10a}$$

$$B_{vA} = B + F\rho_b^2 W^{(2)}_{vA} + F[3\rho_a^2\rho_c^2 - 2\rho_a^2\rho_b^2 - 2\rho_b^2\rho_c^2]W^{(4)}_{vA} + [\rho_a^2(C-B) + \rho_c^2(A-B)]W^{(\mathrm{d})}_{vA} \tag{10b}$$

$$C_{vA} = C + F\rho_c^2 W^{(2)}_{vA} + F[3\rho_a^2\rho_b^2 - 2\rho_a^2\rho_c^2 - 2\rho_b^2\rho_c^2]W^{(4)}_{vA} + [\rho_a^2(B-C) + \rho_b^2(A-C)]W^{(\mathrm{d})}_{vA} \tag{10c}$$

For the $E$-levels the odd-order terms may be important and, in this case, it is necessary to add to the Watson Hamiltonian at least the linear terms

$$\mathbf{H}_{\mathrm{lin}} = \sum_g D_g J_g + \cdots \tag{11}$$

with

$$D_g = F\rho_g W^{(1)}_{vE}. \tag{12}$$

An interesting property of the $W^{(2n)}_{v\sigma}$ coefficients is that [36]

$$W^{(2n)}_{vA} = -2W^{(2n)}_{vE}. \tag{13}$$

[1] This is of course true if the barrier is high and the internal splittings are small or if $\rho$ and/or the rotational quantum number $K$ (associated with the projection of the rotational angular momentum along the symmetry axis of the molecule) are small so that the splittings can be treated as a power series.

If we neglect the denominator correction, it is possible to obtain the "unperturbed" ground-state rotational constants (i.e., without the internal rotation contribution) from the $A$- and $E$-constants as

$$A = \frac{A_A + 2A_E}{3}, \tag{14}$$

and similar equations hold for $B$, and $C$.

In summary, there are two ways to obtain the "unperturbed" rotational constants of the molecule from a PAM analysis [41]: (i) by determining the rotational constants of the $A$-lines and correcting them with the help of Eqs. (10), for results see first line of Table 6, where no denominator correction (i.e. $W^{(\mathrm{d})}_{v\sigma} = 0$) was applied; and *ii*) by determining the rotational constants of the $A$- and $E$-lines using Eq. (14), for results see the second line of Table 6.

### 4.2. Rho-axis method (RAM)

The problem of the PAM is that the $\mathbf{H}^{\mathrm{PAM}}_{v\sigma}$ Hamiltonian, Eq. (9), converges very slowly (especially if the barrier is small). For this reason, it has been proposed to use different axis systems which eliminate the $2F\rho_x p J_x$ term. In the case of a molecule with an (**a b**) symmetry plane (which is the most frequent case treated in the literature up to now and which applies in particular for CMF) and the $I^r$ representation [$(a, b, c) = (z, x, y)$], the Coriolis cross-term $2F\rho_y p J_y$ does not exist. One coordinate axis is coincident with the $\boldsymbol{\rho}$ vector. In the particular case of an (**a b**) symmetry plane (the general case where the frame of the molecule has no plane of symmetry is treated in the Appendix), this corresponds to a rotation about the $c$ axis by an angle $\beta$, which is also called $\theta_{\mathrm{RAM}}$ in the BELGI code [42], given by:

$$\tan\ \beta = \frac{\rho_b}{\rho_a} \tag{15}$$

The Hamiltonian may be written as

$$\mathbf{H}^{\mathrm{RAM}} = \mathbf{H}_{\mathrm{T}} + \mathbf{H}_{\mathrm{R}} + \mathbf{H}_{\mathrm{CD}} + \mathbf{H}_{\mathrm{INT}}, \tag{16}$$

where $\mathbf{H}_{\mathrm{T}}$ is a torsional Hamiltonian, $\mathbf{H}_{\mathrm{R}}$ a rotational Hamiltonian, $\mathbf{H}_{\mathrm{CD}}$ the usual centrifugal distortion Hamiltonian, and $\mathbf{H}_{\mathrm{INT}}$ contains higher-order torsional–rotational interaction terms:

$$\mathbf{H}_{\mathrm{T}} = F(p_\alpha - \rho J_a)^2 + \frac{1}{2}V_3(1 - \cos 3\alpha) + \cdots \tag{17}$$

$$\mathbf{H}_{\mathrm{R}} = A_{\mathrm{RAM}}J_a^2 + B_{\mathrm{RAM}}J_b^2 + C_{\mathrm{RAM}}J_c^2 + D_{ab}(J_aJ_b + J_bJ_a) \tag{18}$$

It is straightforward to establish the relationship between the rotational constants $A$, $B$, $C$ in the principal axis system and the constants $A_{\mathrm{RAM}}$, $B_{\mathrm{RAM}}$, $C_{\mathrm{RAM}}$, and $D_{ab}$ in the rho-axis system using

**Table 6**
Ground-state rotational constants $B^{\mathrm{g}}_{v_\tau=0}$ ($g = a, b, c$) in the PAS of *cis*-methyl formate without taking into account the denominator correction (all values in MHz).

| | $A$ | $B$ | $C$ |
|---|---|---|---|
| From Eq. (10)[a] | 19 982.158 | 6913.968 | 5304.473 |
| From Eq. (14)[b] | 19 982.181(11) | 6914.041(2) | 5304.497(2) |
| "Woods" CAM[c] | 19 982.239(5) | 6914.013(1) | 5304.480(1) |
| "Lille" CAM[d] | 19 982.181(55) | 6914.041(14) | 5304.498(13) |
| ErHam[e] | 19 982.1953(6) | 6914.0397(2) | 5304.4979(2) |
| RAM[f] | 19 985.192 | 6913.205 | 5304.871 |

[a] From $v_\tau = 0$ data of Ref. [57].
[b] From $v_\tau = 0$ data of Refs. [55,57].
[c] Ref. [58], $v_\tau = 0$ data.
[d] Ref. [56], $v_\tau = 0$ data, denominator correction neglected.
[e] Ref. [33], from a fit of $v_\tau = 0$ data, "combined" method, see text.
[f] Ref. [3], from a global fit of $v_\tau = 0$ and 1 data and use of Eq. (20) with experimental values of Ref. [33] for the $\alpha$-constants, see Table 7.

the definition of $\beta$ or by diagonalizing the $3 \times 3$ matrix of RAM rotational constants. In the particular case of an (**a b**) symmetry plane, it gives

$$\tan 2\beta = \frac{2D_{ab}}{A_{\mathrm{RAM}} - B_{\mathrm{RAM}}}. \quad (19)$$

There are different variants of the RAM. From a fit of the spectrum, the following parameters may be derived: $V_3$, $F$, $A_{\mathrm{RAM}}$, $B_{\mathrm{RAM}}$, $C_{\mathrm{RAM}}$, $D_{ab}$, and the modulus $\rho$ (plus higher-order parameters). This is the method chosen in the computer program BELGI [42]. The internal rotation angle $\beta$ is derived from Eq. (19). See the Appendix for the case of a molecule without a plane of symmetry and for the transformation of the PAM parameters into RAM parameters and vice versa. This method is quite efficient for fitting spectra. However, it induces large correlations between the rotational constants and $D_{ab}$, especially if the dataset contains rotational transitions only within the ground torsional state $v_\tau = 0$ (which would allow to float only the potential barrier $V_3$ or the internal rotation constant $F$). In this case, the internal rotation splittings rarely carry enough information to completely break down this correlation. Furthermore, a fit with BELGI is very time consuming for high-$J$ values. For this reason, some authors prefer to transform the PAM rotational constants into RAM rotational constants using the internal rotation angle $\beta$ (and $\gamma$ if the **ρ** vector does not lie in the (**a b**) plane, see Appendix) and to fit the PAM rotational constants. This is the "combined axis method" (CAM) chosen in the effective rotational-torsional Hamiltonian (ErHam) approach [43] as well as in the method chosen by Woods, which was called historically Internal Axis Method (IAM) [39,44], or in the XIAM method [45]. The CAM delivers constants which do not need to be corrected by removing contributions from higher torsional levels as it allows to fit each torsional state separately, see third and fourth lines of Table 6 for the CAM methods and line five for the ErHam method. The results for the ground-state rotational constants derived from the RAM method used in the BELGI code are shown on line six of Table 6. They needed to be corrected to remove the effects of higher excited torsional states, as explained in Section 4.3.

### 4.3. BELGI [42]

In the version BELGI of the RAM, sometimes referred to as a "global approach", all torsional states are included in the matrix associated with the Hamiltonian (up to a certain truncation level carefully checked so that this truncation does not affect the energy levels) and fitted simultaneously. In that sense the internal rotation is treated as a rotation, not as a vibration. This approach is particularly useful when dealing with low barriers (or for torsional levels close to the top of the barrier) where the matrix elements connecting different torsional states are important and cannot be neglected. However, the drawback is that for this reason, the rotational constants derived, after transformation in the PAM, $B^g_{\mathrm{PAM}}$ are "torsionless" because, in BELGI, the torsion is not considered as a vibration but is treated separately. To obtain the ground-state rotational constants $B^g_{v_\tau=0}$, the following correction has to be applied

$$B^g_{v_\tau=0} = B^g_{\mathrm{PAM}} - \frac{1}{2}\alpha^g_\tau, \quad (20)$$

where $\alpha^g_\tau = B^g(v_\tau = 0) - B^g(v_\tau = 1)$ is the vibration–rotation interaction constant corresponding to the torsional vibration. The transformation is given in Table 7 where the first line shows the values of the rotational constants obtained from the RAM analysis [3] and the second line shows the rotational constants transformed into their PAM values, by the diagonalization of the inertia tensor. After applying Eq. (20) to the PAM values, i.e., substracting $1/2\alpha^g_\tau$ derived experimentally from Maeda et al. [33] and reported in the third line of Table 7, one obtains the values for $B^g_{v_\tau=0}$ (fourth line of Table 7).

**Table 7**
Rotational constants (MHz) from the RAM analysis.

| | $A$ | $B$ | $C$ | $D_{ab}$ |
|---|---|---|---|---|
| RAM, $v_\tau$ = e[a] | 17 629.39(21) | 9242.94(13) | 5318.021(78) | –4925.72(4) |
| PAS, $v_\tau$ = e[a,b] | 19 925.58(30) | 6946.75(21) | 5318.021(78) | 0 |
| $\alpha_\tau$(exp)[c] | –119.224(3) | 67.08217(83) | 26.30104(36) | 0 |
| PAS, $v_\tau$ = 0[d] | 19 985.19(30) | 6913.21(21) | 5304.871(78) | 0 |

[a] Experimental "torsionless" values from Ref. [3].
[b] Principal axis system values, obtained by diagonalization of the tensor of the RAM values of previous line.
[c] Ref. [33].
[d] Ground-state values in the principal axis system obtained using Eq. (20) and the data of the two previous lines.

Those ground-state $v_\tau = 0$ values of the rotational constants are also the ones reported in the fourth column of Table 6 as "RAM corrected" derived values.

The agreement between the different sets of rotational constants is fair enough to prove that the method is correct. However, the agreement is not very good for two reasons:

(i) The molecule is considered as a semi-rigid molecule whereas the torsion is a large-amplitude motion, thus Eq. (20) is approximate. Furthermore, the correction applied with Eq. (20) is an estimation because the RAM rotational constants do not only carry the contribution of $v_\tau = 1$ but also from all the torsional stack ($v_\tau = 0, 1, 2, \ldots 9$) because in the CMF molecule quite large $\cos 3\alpha \cos 6\alpha$ terms connect different $v_\tau$'s and those rotation–torsion interaction terms are explicitly present in the Hamiltonian matrices used in BELGI.
(ii) And, more importantly, the rotational constants derived from the RAM analysis are not very accurate because of correlation problems discussed above. Furthermore, $D_{ab}$ is not very accurate in the particular case of CMF. The reduced barrier is actually rather large and **ρ** is small (0.08), thus not much torsional information is transferred to the rotational transitions. The same type of situation occurred with our study of the ester of the dialanine [46], for the case of the methyl group which has the "high" barrier: $D_{ab}$ was not so well determined, so the cosine angles between the PAS and the symmetry axis of the methyl group have also a few degrees discrepancy and the rotational constants have large standard deviations.

### 4.4. Comments on the denominator correction

If the denominator correction is neglected, the unperturbed frequency of a rotational line is given, see Eqs. (13) and (14), by

$$\nu = \frac{\nu_A + 2\nu_E}{3} \quad (21)$$

This is the frequency which would be obtained in the absence of internal rotation and, when fitted, it is in perfect agreement with the unsplit lines. On the other hand, even when all the lines are unsplit, as in $HCOOCD_3$, there is still a non-negligible denominator correction (in MHz): $\Delta A = -1.37$; $\Delta B = -0.76$ and $\Delta C = 2.13$ (calculated with $W_0^{(d)} \approx 0.0299$ obtained by interpolation from Ref. [38]). Thus, it seems that this correction should not be taken into account during the structure determination of CMF. A further argument supporting this comes from the following analysis of the pseudo-inertial defect.

At equilibrium, CMF possesses a plane of symmetry with one pair of equivalent out-of-plane hydrogen atoms. The equilibrium distance $d^e_{HH}$ between the hydrogens of this pair is given by

$$2P^e_c = m_H(d^e_{HH})^2 = I^e_a + I^e_b - I^e_c = I^0_a + I^0_b - I^0_c + \Delta_{vib} \quad (22)$$

where $\Delta_{vib}$ is the vibrational contribution to the inertial defect. It is often assumed that the anharmonic contribution to $\Delta_{vib}$ may be neglected, as for planar molecules [47]. Thus, $\Delta_{vib}$ might be easily calculated from the harmonic force field and $d^e_{HH}$ may be derived using Eq. (22). Unfortunately, as seen by comparing the harmonic contribution $\Delta_{harm}$ to $\Delta_{vib}$ in Table 8, this assumption is not a valid one.

Another approximation which is often made is to assume that $\Delta_{vib}$ does not change upon the isotopic substitution $CH_3 \rightarrow CD_3$ [48]. As can be seen in Table 8, which shows the vibrational contribution for different isotopologues of CMF, this assumption is not verified either.

On the other hand, once the cubic force field in normal coordinates is known, it is straightforward to calculate $\Delta_{vib}$ and, as this correction is small, it is possible to determine the $d^e_{HH}$ distance. The results are reported in Table 8 with and without the denominator correction. The comparison of these results with the *ab initio* equilibrium value, $d^e_{HH}$ = 1.7711 Å, confirms that the denominator correction has to be left out for a structure determination. Note that the value from $HCOOCH_2D_s$ is an outlier, it is due to the fact that the *A* rotational constant of this isotopologue is not accurate. This is further discussed in the next section. Dropping this value decreases the standard deviation of the mean of the $d^e_{HH}$ values from 0.0010 to 0.0004 Å.

A final point has to be discussed. The denominator correction introduces a non-diagonal term in the rotational Hamiltonian of the form [40]

$$\frac{1}{2}\rho_a\rho_b(A+B-2C)W^{(d)}_{v\sigma}(J_aJ_b + J_bJ_a). \quad (23)$$

This induces a rotation of axes of 0.004° which has a negligible effect on the rotational constants.

**Table 8**
Inertial defects (in uÅ$^2$) and $d^e_{HH}$ (in Å) for the symmetrical isotopologues of *cis*-methyl formate.

| Species | $2P^{0a}_c$ | $2P^{eb}_c$ | $\Delta_{vib}$[c] | $\Delta_{harm}$[d] | $d^e_{HH}$ | |
|---|---|---|---|---|---|---|
| | | | | | [e] | [f] |
| $HCOOCH_3$ | 3.1124 | 3.1652 | 0.0567 | 0.0232 | 1.7722 | 1.7653 |
| $DCOOCH_3$ | 3.1152 | 3.1647 | 0.0535 | 0.0191 | 1.7720 | 1.7657 |
| $HCOOCH_2D_s$ | 3.1585 | 3.1752 | 0.0207 | −0.0007 | 1.7750 | |
| $HCOOCD_3$ | 6.3284 | 6.3301 | 0.0055 | −0.0224 | 1.7728 | 1.7650 |
| $H^{13}COOCH_3$ | 3.1116 | 3.1649 | 0.0573 | 0.0236 | 1.7721 | 1.7658 |
| $HCOO^{13}CH_3$ | 3.1102 | 3.1646 | 0.0584 | 0.0247 | 1.7720 | 1.7654 |
| $HC^{18}OOCH_3$ | 3.1088 | 3.1652 | 0.0601 | 0.0296 | 1.7722 | 1.7657 |
| $HCO^{18}OCH_3$ | 3.1090 | 3.1656 | 0.0605 | 0.0224 | 1.7723 | 1.7652 |
| $HCOOCD_2H$ | 6.2772 | 6.3200 | 0.0463 | 0.0019 | 1.7714 | |
| Mean | | | | | 1.7724(10)[g] | 1.7654(3) |

[a] $2P^0_c = I^0_a + I^0_b - I^0_c$, without denominator correction (derived from the "unperturbed" experimental ground-state rotational constants, $A_0$, $B_0$, $C_0$ from Table 9).
[b] $2P^e_c = I^e_a + I^e_b - I^e_c$, without denominator correction (derived from the semi-experimental equilibrium rotational constants $A_{SE}$, $B_{SE}$, $C_{SE}$ from Table 9).
[c] $\Delta_{vib} = 2P^e_c - 2P^0_c$.
[d] Harmonic contribution to $\Delta_{vib}$, calculated from the MP2/VTZ harmonic force field.
[e] Calculated from $2P^e_c$ without denominator correction.
[f] Calculated from $2P^e_c$ with denominator correction.
[g] $r^{BO}_e$ value: 1.7711 Å, see Table 1.

## 5. Semi-experimental equilibrium structure, $r^{SE}_e$

The theoretical α-constants deduced from the *ab initio* cubic force field were combined with the known experimental ground-state rotational constants $A_0$, $B_0$, $C_0$ of Table 9 to yield the semi-experimental equilibrium rotational constants $A_{SE}$, $B_{SE}$, $C_{SE}$. For each isotopologue, it was checked that Eqs. (10) and (14) and the CAM methods give compatible results when internal rotation splittings are present in the spectrum. Table 9 also shows the results for various isotopologues of CMF. When there is no internal rotation splitting (–$CD_3$, –$CH_2D$, and –$CHD_2$ species), a standard Watson Hamiltonian was used. These derived semi-experimental equilibrium constants were corrected for a small magnetic effect using the experimental *g*-constants of Ref. [49]. The corrected values of the rotational constants are given by the relation [50]

$$B^{\xi}_{corr} = \frac{B^{\xi}_{exp}}{1 + \frac{m}{M_p}g_{\xi\xi}} \quad (24)$$

where $g_{\xi\xi}$ is expressed in units of the nuclear magneton, $m$ is the electron mass, $M_p$ the proton mass, and $\xi = a, b, c$. This correction is found to be rather small ($\Delta A$ = 1.38 MHz, $\Delta B$ = 0.15 MHz and $\Delta C$ = 0.05 MHz for the parent species) and does not significantly affect the structure. The equilibrium structure was calculated from a weighted least-squares fit of the semi-experimental moments of inertia. As it is difficult to estimate the precision of the moments of inertia, the iteratively reweighted least-squares method was used [51]. At the end of the iterations, similar weights are obtained for all moments of inertia. However, note that the residuals are larger for

**Table 9**
Experimental ground-state rotational constants, MP2/VTZ rovibrational corrections, and semi-experimental equilibrium rotational constants (all values in MHz).

| Isotopologue[a] | Ground-state | | | Rovib. corrections | | | Semi-experimental[b] | | | Residuals of the fit[c] | | | Ref.[d] |
|---|---|---|---|---|---|---|---|---|---|---|---|---|---|
| | $A_0$ | $B_0$ | $C_0$ | $A_e - A_0$ | $B_e - B_0$ | $C_e - C_0$ | $A_{SE}$ | $B_{SE}$ | $C_{SE}$ | $A_{SE} - A_{calc}$ | $B_{SE} - B_{calc}$ | $C_{SE} - C_{calc}$ | |
| $HCOOCH_3$ | 19 982.18 | 6914.04 | 5304.50 | 35.69 | 105.04 | 67.34 | 20019.25 | 7019.23 | 5371.88 | 0.03 | −0.02 | −0.01 | [3,33] |
| $DCOOCH_3$ | 18 475.71 | 6768.41 | 5109.70 | 36.94 | 101.82 | 63.45 | 18513.83 | 6870.37 | 5173.19 | 0.13 | 0.01 | −0.01 | [11] |
| $HCOOCH_2D_s$ | 19 921.59 | 6415.27 | 5004.27 | 52.18 | 90.39 | 59.16 | 19975.14 | 6505.79 | 5063.48 | −1.86 | −0.01 | 0.27 | [53] |
| $HCOOCH_2D_a$ | 18 516.73 | 6730.19 | 5164.96 | 38.45 | 96.93 | 63.58 | 18556.37 | 6827.26 | 5228.58 | 0.71 | 0.34 | −0.07 | [53] |
| $HCOOCD_3$ | 17 261.81 | 6101.92 | 4778.01 | 53.09 | 81.36 | 54.07 | 17315.93 | 6183.39 | 4832.12 | −0.58 | −0.11 | 0.09 | [4] |
| $H^{13}COOCH_3$ | 19 798.73 | 6864.76 | 5262.52 | 32.78 | 103.75 | 66.25 | 19832.87 | 6968.66 | 5328.82 | 0.01 | 0.01 | −0.02 | [33] |
| $HCOO^{13}CH_3$ | 19 765.12 | 6742.65 | 5188.08 | 32.61 | 102.61 | 65.94 | 19799.08 | 6845.40 | 5254.06 | −0.35 | 0.03 | −0.04 | [10] |
| $HC^{18}OOCH_3$ | 19 525.80 | 6617.19 | 5097.25 | 37.58 | 99.10 | 64.31 | 19564.70 | 6716.43 | 5161.61 | 0.38 | −0.02 | 0.03 | [1] |
| $HCO^{18}OCH_3$ | 19 323.00 | 6848.97 | 5219.01 | 32.71 | 102.28 | 64.88 | 19357.00 | 6951.40 | 5283.94 | 0.10 | −0.00 | 0.03 | [61] |
| $HCOOCHD_2s$ | 17 281.94 | 6540.60 | 5041.99 | 38.62 | 92.93 | 60.73 | 17321.60 | 6633.67 | 5102.76 | 1.35 | 0.22 | −0.05 | [62] |
| $HCOOCHD_2a$ | 18 482.05 | 6261.07 | 4884.21 | 53.76 | 83.51 | 56.22 | 18537.00 | 6344.70 | 4940.47 | −1.24 | −0.64 | 0.00 | [62] |

[a] s = atom in the symmetry plane; a = atom out of the symmetry plane.
[b] $A_{SE} = A_0$ + rovibrational correction + electronic effect (see text).
[c] Residuals of the least-squares fit, values calculated using parameters of last column of Table 10.
[d] Reference for the ground-state rotational spectra.

**Table 10**
Structures of *cis*-methyl formate (bond lengths in Å, angles in degrees).

| Parameter[a] | $r_s$ [4][b] | $r_a$ [12][b,c] | MP2/VQZ [13] | $r_e^{BO}$(I)[d] | $r_e^{BO}$(II)[d] | $r_e^{SE}$[e] |
|---|---|---|---|---|---|---|
| $r(C_m–O)$ | 1.437(10) | 1.435(3) | 1.4344 | 1.4338 | 1.4355 | 1.4341(5) |
| $r(O–C_c)$ | 1.334(10) | 1.340(2) | 1.3370 | 1.3343 | 1.3347 | 1.3345(4) |
| $r(C_m–H_s)$ | 1.086(15) | | 1.0817 | 1.0834 | 1.0837 | 1.0793(10) |
| $r(C_m–H_a)$ | 1.086(15) | | 1.0851 | 1.0868 | 1.0872 | 1.0871(3) |
| $r(C_c–H)$ | 1.101(10) | 1.122(12) | 1.0922 | 1.0931 | 1.0934 | 1.0930(5) |
| $r(C=O)$ | 1.200(10) | 1.202(2) | 1.2035 | 1.1997 | 1.2008 | 1.2005(5) |
| $\angle(COC)$ | 114.8(10) | 115.9(5) | 114.0 | 114.360 | 114.411 | 114.32(4) |
| $\angle(CCH_s)$ | 108.2(16) | | 105.5 | 105.628 | 105.572 | 106.05(16) |
| $\angle(CCH_a)$ | 108.2(16) | | 110.3 | 110.217 | 110.125 | 110.19(2) |
| $\angle(OCH)$ | 109.3(10) | 109.3(10) | 109.2 | 109.569 | 109.653 | 109.60(5) |
| $\angle(OCO)$ | 125.9(10) | 125.4(5) | 125.6 | 125.525 | 125.467 | 125.50(5) |
| $\tau(H_aCOC)$ | | | 60.3 | 60.259 | 60.248 | 60.28(3) |

[a] m stands for methyl, c for carbonyl, s for symmetric (in-plane) and a for asymmetric (out-of-plane), see Fig. 1.
[b] Methyl group assumed to be symmetric.
[c] Electron diffraction structure.
[d] See Table 1.
[e] Semi-experimental equilibrium structure, see text.

the $-CH_2D$ and $CHD_2$ species, see Table 9. The semi-experimental equilibrium structure is in excellent agreement with the *ab initio* Born–Oppenheimer equilibrium structure approximated at the CCSD(T)/V5Z level, except for the distance $r(CH_s)$ and the angle $\angle(CCH_s)$. These two parameters are highly correlated, correlation coefficient $\rho = -0.9737$ with a rather large condition number, $\kappa = 511$. This correlation may be partly explained by the fact that the in-plane hydrogen of the methyl group is close to the principal *b*-axis, $b(H_s) = -0.246$ Å. It is indeed well established that it is difficult to obtain an accurate value for a small coordinate [52]. Furthermore, the residuals of the fit are particularly large for the species which determine the position of $H_s$, i.e. the $-CH_2D_s$ species (see Table 9). One possible explanation is that there is a weak interaction between the levels of the $-CH_2D_s$ and the $-CH_2D_a$ species which happen to be quite close [53]. This explanation also applies for the $-CHD_2$ species. However, the fit of the rotational transitions to a standard Watson Hamiltonian is good from a statistical point of view and the quartic centrifugal distortion constants do not appear to be significantly perturbed. They have indeed the expected order of magnitude and they are furthermore close to the *ab initio* values.

## 6. Discussion

It is worth noting that the different structures ($r_s$, $r_a$, $r_e$(MP2/VQZ),...) are in fair agreement, except for the structure of the methyl group. Actually, the methyl group is found to be highly asymmetric. with $r(C_m–H_a) - r(C_m–H_s) = 0.0035$ Å and $\angle(CCH_a) - \angle(CCH_s) = 4.55°$. The $r(C_c–H)$ value at 1.093 Å is large but smaller than the value found in HCOOH, 1.098 Å [54]. Likewise, the $r(O–C_c)$ value at 1.334 Å is smaller than in HCOOH where it is 1.347 Å. On the other hand, the $r(C=O)$ value at 1.200 Å is larger than in HCOOH, 1.192 Å.

It is interesting to check whether the internal rotation parameters are compatible with the equilibrium structure. The equilibrium value of the principal moment of inertia of the methyl group calculated from the equilibrium structure is $I_{\alpha'} = 3.198$ uÅ$^2$. $I_\alpha$ can be obtained from the experimental value of $|\boldsymbol{\rho}| = 0.0842153$ and the derived values of the direction cosines [3], see Eq. (4), it gives $I_{\alpha'} = 3.22$ uÅ$^2$, not too far from the equilibrium value. However, it gives $F = 5.648$ cm$^{-1}$, see Eq. (5); rather far from the experimental value of 5.505 cm$^{-1}$ [3]. On the other hand, starting from $F_{exp}$, which gives $rI_{\alpha'}$ one deduces $I_{\alpha'} = 3.315$ uÅ$^2$. This discrepancy indicates that the non-rigidity effects are important for $I_\alpha$ and that it is better to consider $I_\alpha$ as a fitting parameter.

It is also possible to compare the values obtained for the internal rotation angle $\theta = \angle(i, a)$. The experimental value deduced from the RAM analysis is $\theta = 52.989°$, rather far from the equilibrium value $\angle(a, OC) = 58.07°$. However, the methyl top is quite asymmetric. If we take into account the asymmetry, we get from the equilibrium structure $\angle(i, a) = \angle(a, OC) - \angle(i, OC) = 54.64°$ (where $\angle(i, OC) = 180 - \angle(OCH_s) - \angle(i, CH_s)$). The discrepancy is strongly reduced but not eliminated. In conclusion, the internal rotation parameters $I_\alpha$ and $\theta$ (or $|\boldsymbol{\rho}|$ and $\beta$) are significantly affected by non-rigidity effects and cannot be used for an accurate structure determination. Moreover, the values of these parameters are sensitive to the approximations made during the analysis and different analyses often give incompatible parameters.

## Acknowledgments

The authors would like to thank the French "réseau formation-recherche PECO-NEI" for travel grants with Hungary, and the European Associate Laboratory "HighRes". Part of this work is supported by the French ANR-08-BLAN TopModel grant. The work performed in Hungary was supported by the Hungarian Scientific Research Fund (OTKA Grant T72885). J.D. thanks the Barbara Mez-Starck foundation for financial support. The authors would also like to thank Dr. J.T. Hougen for numerous discussions during the work.

## Appendix A:. Transformation formulas

The principal axis system (PAS) used in the principal axis method (PAM) is defined by three orthonormal unit vectors **a**, **b**, **c**. In addition, we define an unit vector **i** in the direction of the internal axis, see Fig. 2. To define the position of **i** in the PAS, we use spherical coordinates: **i** is projected onto the (**b c**) plane giving *y*: $\angle(y, \mathbf{b}) = \varphi$ and $\angle(\mathbf{a}, \mathbf{i}) = \theta$ with $0 \leqslant \theta \leqslant 180°$ and $0 \leqslant \varphi \leqslant 360°$.

The direction cosines of **i** are: $(\lambda_a, \lambda_b, \lambda_c) = (\cos\theta, \sin\theta\cos\varphi, \sin\theta\sin\varphi)$.

We also define the vector $\boldsymbol{\rho} = (\rho_a, \rho_b, \rho_c)$ where

$$\rho_g = \lambda_g \frac{I_\alpha}{I_g} (g = a,\ b,\ c) \tag{A.1}$$

hence

$$\rho = \frac{I_\alpha}{K_1} (A\cos\theta,\ B\sin\theta\ \cos\varphi,\ C\sin\theta\ \sin\varphi) \tag{A.2}$$

with

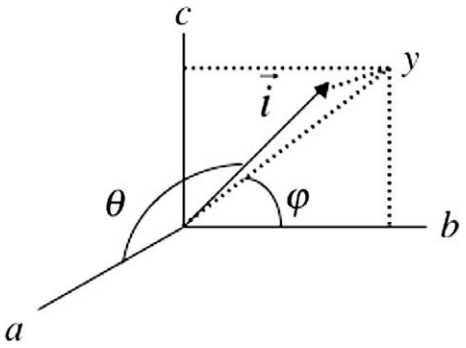


**Fig. 2.** Definition of the internal rotation angles $\theta = \angle(\mathbf{a}, \mathbf{i})$ and $\varphi = \angle(y, \mathbf{b})$ and of the vector **i** in the PAM ($y$ is the projection of **i** onto the (**b c**) plane.

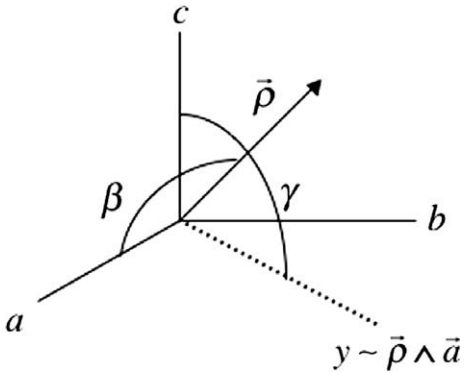


**Fig. 3.** Definition of the internal rotation angles $\beta = \angle(\mathbf{a}, \boldsymbol{\rho})$ and $\gamma = \angle(\mathbf{c}, y)$ and of the vector **ρ** in the RAM. The half line $y$ is perpendicular to the plane defined by the **a**-axis and **ρ** and points in the direction such that **ρ**, **a**, and $y$ form a right-handed system ($\wedge$ means vector product.

$$K_1 = \frac{h}{8\pi^2} = 505379.07 \text{ MHz uA}^2 \tag{A.3}$$

In the rho-axis method (RAM), we define two new angles $\beta$ and $\gamma$. $\beta$ is the angle between **ρ** and the principal axis **a**: $\beta = \angle(\mathbf{a}, \boldsymbol{\rho})$, see Fig. 3. Note that the angle $\beta$ is often called $\theta_{\text{RAM}}$ by people using BELGI. $\gamma$ is the angle between the principal axis **c** and the half line $y$, which is perpendicular to the plane defined by **a** and **ρ**, and points in the direction such that **ρ**, **a**, and $y$ form a right-handed system: i.e. define the new axis $y$ in the (**b c**) plane along the direction **ρ**∧**a** where $\wedge$ means cross product. $\gamma = \angle(\mathbf{c}, y)$ and the vector **ρ** can now be defined with these angles

$$\rho = \rho(\cos\beta, -\sin\beta\ \cos\gamma,\ \sin\beta\ \sin\gamma) \tag{A.4}$$

Likewise, the vector **i** can be written

$$\mathbf{i} = \frac{\rho}{I_\alpha}(I_a\cos\beta,\ -I_b\sin\beta\ \cos\gamma,\ I_c\sin\beta\ \sin\gamma) \tag{A.5}$$

And the rotation matrix which rotates the PAS towards the rho-axis system (RAS) may be written

$$\mathbf{R} = \begin{pmatrix} \cos\beta & -\sin\beta\ \cos\gamma & \sin\beta\ \sin\gamma \\ \sin\beta & \cos\beta\ \cos\gamma & -\cos\beta\ \sin\gamma \\ 0 & \sin\gamma & \cos\gamma \end{pmatrix} \tag{A.6}$$

In the frequent case where **ρ** lies in the (**a b**) plane, $\gamma = 0$.

*A.1. PAM → RAM*

It is easy to transform the PAM parameters into RAM parameters

$$\tan\beta = 2\frac{\sqrt{\rho_b^2 + \rho_c^2}}{\rho_a} = \frac{1}{A}\sqrt{B^2\cos^2\varphi + C^2\sin^2\varphi}\ \tan\theta \tag{A.7}$$

$$\tan\gamma = -\frac{\rho_c}{\rho_b} = -\frac{C}{B}\tan\varphi \tag{A.8}$$

and

$$\rho = \frac{I_\alpha}{K_1}\sqrt{A^2\cos^2\theta + (B^2\cos^2\varphi + C^2\sin^2\varphi)\sin^2\theta} \tag{A.9}$$

Finally,

$$r = 1 - \sum_g \lambda_g^2\left(\frac{I_\alpha}{I_g}\right)^2 = 1 - \boldsymbol{\rho}\cdot\mathbf{i} \tag{A.10}$$

$$F = \frac{K_1}{rI_\alpha} = \left\{\frac{I_\alpha}{K_1}[A\cos^2\theta + (B\cos^2\varphi + C\sin^2\varphi)\sin^2\theta]\right\}^{-1} \tag{A.11}$$

*A.2. RAM → PAM*

$$\tan\theta = \frac{\sqrt{i_b^2 + i_c^2}}{i_a} = \frac{1}{I_a}\sqrt{I_b^2\cos^2\gamma + I_c^2\sin^2\gamma}\cdot\tan\beta \tag{A.12}$$

$$\tan\varphi = \frac{i_c}{i_b} = -\frac{I_c}{I_b}\tan\gamma \tag{A.13}$$

$$I_\alpha = \rho\sqrt{I_a^2\cos^2\beta + (I_b^2\cos^2\gamma + I_c^2\sin^2\gamma)\sin^2\beta} \tag{A.14}$$

## References

[1] C.E. Blom, Hs.H. Günthard, Chem. Phys. Lett. 84 (1981) 267–271.
[2] M.T. Muckle, J.L. Neill, D.P. Zaleski, B. Pate, M.C. McCarthy, S. Spezzano, V. Lattanzi, A.J. Remijan, in: International Symposium on Molecular Spectroscopy, 64th Meeting, June 22–26, 2009, Columbus, USA.
[3] V. Ilyushin, A. Kryvda, E. Alekseev, J. Mol. Spectrosc. 255 (2009) 32–38.
[4] R.F. Curl, J. Chem. Phys. 30 (1959) 1529–1536.
[5] J. Chao, K.R. Hall, K.N. Marsh, R.C. Wilhoit, J. Phys, Chem. Ref. Data 15 (1986) 1369–1436.
[6] E. Churchwell, G. Winnewisser, Astron. Astrophys. 45 (1975) 229–231.
[7] A. Nummelin, P. Bergman, A. Hjalmarson, P. Friberg, W.M. Irwine, T.J. Millar, M. Ohishi, S. Saito, Astrophys. J. Suppl. Ser. 117 (1998) 427–529.
[8] A. Horn, H. Møllendal, O. Sekiguchi, E. Uggerud, H. Roberts, E. Herbst, A.A. Viggiano, T.D. Fridgen, Astrophys. J. 611 (2004) 605–614.
[9] K. Kobayashi, K. Ogata, S. Tsunekawa, S. Takano, Astrophys. J. 657 (2007) L17–L19.
[10] M. Carvajal, L. Margulès, B. Tercero, K. Demyk, I. Kleiner, J.-C. Guillemin, V. Lattanzi, A. Walters, J. Demaison, G. Wlodarczak, T.R. Huet, H. Møllendal, V.V. Ilyushin, J. Cernicharo, Astron. Astrophys. 500 (2009) 1109–1118.
[11] L. Margulès, T.R. Huet, J. Demaison, M. Carvajal, I. Kleiner, H. Møllendal, B. Tercero, N. Marcelino, J. Cernicharo, Astrophys. J., submitted for publication.
[12] S. Cradock, D.W.H. Rankin, J. Mol. Struct. 69 (1980) 145–149.
[13] M.L. Senent, M. Villa, F.J. Meléndez, R. Dominguez-Gómez, Astrophys. J. 627 (2005) 567–576.
[14] C. Møller, M.S. Plesset, Phys. Rev. 46 (1934) 618–622.
[15] G.D. Purvis III, R.J. Bartlett, J. Chem. Phys. 76 (1982) 1910–1918.
[16] K. Raghavachari, G.W. Trucks, J.A. Pople, M. Head-Gordon, Chem. Phys. Lett. 157 (1989) 479–483.
[17] T.H. Dunning Jr., J. Chem. Phys. 90 (1989) 1007–1023.
[18] T.J. Lee, G.E. Scuseria, in: S.R. Langhoff (Ed.), Quantum Mechanical Electronic Structure Calculations with Chemical Accuracy, Kluwer, Dordrecht, 1995, pp. 47–108.
[19] J. Demaison, A.G. Császár, A. Dehayem-Kamadjeu, J. Phys. Chem. A 110 (2006) 13609–13617.
[20] D.E. Woon, T.H. Dunning Jr., J. Chem. Phys. 103 (1995) 4572–4585.
[21] Basis sets were obtained from the Extensible Computational Chemistry Environment Basis Set Database, Version 02/02/06, as developed and distributed by the Molecular Science Computing Facility, Environmental and Molecular Sciences Laboratory which is part of the Pacific Northwest Laboratory, P.O. Box 999, Richland, Washington 99352, USA, and funded by the U.S. Department of Energy. The Pacific Northwest Laboratory is a multi-program laboratory operated by Battelle Memorial Institute for the U.S. Department of Energy under contract DE-AC06-76RLO 1830. Contact David Feller or Karen Schuchardt for further information.
[22] A.G. Császár, W.D. Allen, J. Chem. Phys. 104 (1996) 2746–2748.
[23] L. Margulès, J. Demaison, H.D. Rudolph, J. Mol. Struct. 599 (2001) 23–30.
[24] MOLPRO 2000 is a package of ab initio programs written by H.-J. Werner and P.J. Knowles, with contributions from R.D. Amos, A. Bernhardsson, A. Berning, P. Celani, D.L. Cooper, M.J.O. Deegan, A.J. Dobbyn, F. Eckert, C. Hampel, G.

Hetzer, T. Korona, R. Lindh, A.W. Lloyd, S.J. McNicholas, F.R. Manby, W. Meyer, M.E. Mura, A. Nicklass, P. Palmieri, R. Pitzer, G. Rauhut, M. Schütz, H. Stoll, A.J. Stone, R. Tarroni, T. Thorsteinsson. See P.J. Knowles, C. Hampel, H.-J. Werner, J. Chem. Phys. 112 (2000) 3106–3107.
[25] M.J. Frisch, G.W. Trucks, H.B. Schlegel, G.E. Scuseria, M.A. Robb, J.R. Cheeseman, J.A. Montgomery Jr., T. Vreven, K.N. Kudin, J.C. Burant, J.M. Millam, S.S. Iyengar, J. Tomasi, V. Barone, B. Mennucci, M. Cossi, G. Scalmani, N. Rega, G.A. Petersson, H. Nakatsuji, M. Hada, M. Ehara, K. Toyota, R. Fukuda, J. Hasegawa, M. Ishida, T. Nakajima, Y. Honda, O. Kitao, H. Nakai, M. Klene, X. Li, J.E. Knox, H.P. Hratchian, J.B. Cross, C. Adamo, J. Jaramillo, R. Gomperts, R.E. Stratmann, O. Yazyev, A.J. Austin, R. Cammi, C. Pomelli, J.W. Ochterski, P.Y. Ayala, K. Morokuma, G.A. Voth, P. Salvador, J.J. Dannenberg, V.G. Zakrzewski, S. Dapprich, A.D. Daniels, M.C. Strain, O. Farkas, D.K. Malick, A.D. Rabuck, K. Raghavachari, J.B. Foresman, J.V. Ortiz, Q. Cui, A.G. Baboul, S. Clifford, J. Cioslowski, B.B. Stefanov, G. Liu, A. Liashenko, P. Piskorz, I. Komaromi, R.L. Martin, D.J. Fox, T. Keith, M.A. Al-Laham, C.Y. Peng, A. Nanayakkara, M. Challacombe, P.M.W. Gill, B. Johnson, W. Chen, M.W. Wong, C. Gonzalez, J.A. Pople, Revision D.01, Gaussian, Inc., Wallingford, CT, 2004.
[26] J. Demaison, Mol. Phys. 105 (2007) 3109–3138.
[27] R.A. Kendall, T.H. Dunning Jr., R.J. Harrison, J. Chem. Phys. 96 (1992) 6796–6806.
[28] A.G. Császár, in: P.v.R. Schleyer, N.L. Allinger, T. Clark, J. Gasteiger, P.A. Kollman, H.F. Schaefer III, P.R. Schreiner (Eds.), The Encyclopedia of Computational Chemistry, vol. 1, Wiley, Chichester, 1998, pp. 13–30.
[29] C. Puzzarini, G. Cazzoli, J. Mol. Spectrosc. 240 (2006) 260–264.
[30] W.D. Allen, A.G. Császár, J. Chem. Phys. 98 (1993) 2983–3015.
[31] W. Schneider, W. Thiel, Chem. Phys. Lett. 157 (1989) 367–373.
[32] D. Papousek, M.R. Aliev, Molecular Vibrational–Rotational Spectra, Elsevier, Amsterdam, 1982.
[33] A. Maeda, F.C. De Lucia, E. Herbst, J. Mol. Spectrosc. 251 (2008) 293–300.
[34] V. Szalay, A.G. Császár, M.L. Senent, J. Chem. Phys. 117 (2002) 6489–6492.
[35] C.C. Lin, J.D. Swalen, Rev. Mod. Phys. 31 (1959) 841–892.
[36] D.R. Herschbach, J. Chem. Phys. 31 (1959) 91–108.
[37] T. Pedersen, Mol. Phys. 32 (1976) 407–418.
[38] J.E. Wollrab, Rotational Spectra and Molecular Structure, Academic Press, New York, 1967.
[39] B.P. Van Eijck, J. van Opheusden, M.M.M. van Schaik, E. van Zoeren, J. Mol. Spectrosc. 86 (1981) 465–479.
[40] D. Stelman, J. Chem. Phys. 41 (1964) 2111–2115.
[41] R.J. Lavrich, D.F. Plusquellic, R.D. Suenram, G.T. Fraser, A.R. Hight Walker, J. Chem. Phys. 118 (2003) 1253–1265.
[42] J.T. Hougen, I. Kleiner, M. Godefroid, J. Mol. Spectrosc. 163 (1994) 559–583.
[43] P. Groner, J. Mol. Spectrosc. 156 (1992) 164–189.
[44] R.C. Woods, J. Mol. Spectrosc. 21 (1966) 4–24.
[45] H. Hartwig, H. Dreizler, Z. Naturforsch. 51a (1996) 923–932.
[46] D.F. Plusquellic, I. Kleiner, J. Demaison, R.D. Suenram, R.J. Lavrich, F.J. Lovas, G.T. Fraser, V.V. Ilyushin, J. Chem. Phys. 125 (2006). 104312-1-13.
[47] D.R. Herschbach, V.W. Laurie, J. Chem. Phys. 35 (1961) 458–463.
[48] V.W. Laurie, J. Chem. Phys. 28 (1958) 704–706.
[49] J.H.S. Wang, W.H. Flygare, J. Chem. Phys. 53 (1970) 4479–4485.
[50] W. Gordy, R.L. Cook, Microwave Molecular Spectra, Wiley, New York, 1984 (Chapter XI).
[51] L.C. Hamilton, Regression with Graphics, Belmont, CA, 1992 (Chapter 6).
[52] J. Demaison, J.D. Rudolph, J. Mol. Spectrosc. 215 (2002) 78–84.
[53] L. Margulès, L.C. Coudert, H. Møllendal, J.-C. Guillemin, T.R. Huet, R. Janecková, J. Mol. Spectrosc. 254 (2009) 55–68.
[54] J. Demaison, M. Herman, J. Liévin, J. Chem. Phys. 126 (2007) 164305/1–164305/9.
[55] G.M. Plummer, E. Herbst, F.C. De Lucia, G.A. Blake, Astrophys. J. Suppl. Ser. 60 (1986) 949–961.
[56] J. Demaison, D. Boucher, A. Dubrulle, B.P. Van Eijck, J. Mol. Spectrosc. 102 (1983) 260–263.
[57] G.M. Plummer, G.A. Blake, E. Herbst, F.C. De Lucia, Astrophys. J. Suppl. Ser. 55 (1984) 633–656.
[58] A. Bauder, J. Phys. Chem. Ref. Data 8 (1979) 583–618.
[59] J. Demaison, A.G. Császár, I. Kleiner, H. Møllendal, J. Phys. Chem. A 111 (2007) 2574–2586.
[60] J. Demaison, M. Herman, J. Liévin, Int. Rev. Phys. Chem. 26 (2007) 391–420.
[61] L. Margulès, R. Motiyenko, M. Carvajal, I. Kleiner, private communication.
[62] L. Margulès, R. Motiyenko, L. Coudert, in press.